Verificación estructural de buques mediante análisis hidroelástico dinámico basado en la reducción de la matriz modal

Structural assessment of vessels by dynamic hydroelastic analysis based on modal matrix reduction

Antonio José Lorente López, Departamento de Física Aplicada y Tecnología Naval, Universidad Politécnica de Cartagena
Julio García Espinosa, Departamento de Arquitectura, Construcción y Sistemas Oceánicos y Navales, Universidad Politécnica de Madrid
José Enrique Gutiérrez Romero, Departamento de Física Aplicada y Tecnología Naval, Universidad Politécnica de Cartagena
Borja Serván Camas, Centre Internacional de Mètodes Numèrics en Enginyeria (CIMNE)
Pablo Romero Tello, Departamento de Física Aplicada y Tecnología Naval, Universidad Politécnica de Cartagena

RESUMEN

El diseño de un buque o artefacto marino se realiza con el objetivo de garantizar una larga vida útil. Uno de los elementos clave a la hora de alcanzar este objetivo es su estructura, pues es la encargada de soportar los esfuerzos enormemente desfavorables propios de alta mar.

El objetivo de este trabajo es presentar un método de evaluación estructural de detalle mediante la aplicación de un modelo hidroelástico dinámico [1] que permite la verificación estructural reduciendo el tiempo de cálculo sin perder precisión, pues los procedimientos actuales requieren de un estudio detallado de cada condición de carga, lo que implica gran cantidad de horas de simulación y alto coste computacional.

En este modelo se proyecta la solución estructural de alta fidelidad sobre la base modal para obtener la matriz modal del sistema y extender los operadores de amplitud de respuesta (RAO) a las respuestas modales de la estructura (MRAO). Conservando los modos propios que preserven la mayor parte de la energía elástica estructural, se consigue reducir notablemente el número de grados de libertad. Este modelo reducido ha sido implementado y acoplado en el dominio del tiempo dentro del programa de comportamiento en la mar SeaFEM, permitiendo analizar rápidamente la respuesta

de una estructura frente a gran cantidad de casos de carga [2]. Este trabajo muestra el primer caso de aplicación a un buque.

ABSTRACT

During the design of a vessel or marine artefact, one of the main objectives is to ensure a long service life. The structure of these artefacts is essential to achieve this goal, as it is responsible for withstanding the extremely unfavourable stresses of the high seas.

The aim of this paper is to present a method of detailed structural assessment by applying a dynamic hydroelastic model [1] that allows structural verification by greatly reducing the calculation time without losing accuracy. The current procedures used for this purpose require a detailed study of each loading condition, which implies many simulation hours and high computational cost.

In this model, the high-fidelity structural solution is projected onto the modal basis to get the system modal matrix and extend the response amplitude operators (RAO) to the modal response amplitude operators (MRAO) of the structure. By retaining only those eigenmodes that preserve most of the structural elastic energy, the number of structural degrees of freedom can be significantly reduced. This reduced model has been implemented and coupled in the time domain with the seakeeping software SeaFEM, enabling quick analysis of a large number of load cases of the structure [2]. In this work, the first case study of a ship is presented.

1. INTRODUCTION TO THE HYDROELASTICITY MODEL

1.1. Hydroelasticity model

The methodology proposed for verifying marine structures is based on direct hydro-elastic calculation -time domain- using a full-length detailed Finite Element (FE) model. In this section, we first outline the details of the general methodology. The following sections offer specific indications on its application in strength assessment and fatigue assessment.

The hydro-elastic calculation procedure here proposed is based on the methodology presented in reference [1]. In that reference, a strongly coupled hydro-elastic model is introduced, implemented within the SeaFEM software. The fluid domain is solved using a time-domain wave diffraction-radiation solver based on the Finite Element Method (FEM) [3]. The structure is modelled using the FEM and assuming it operates in the linear-elastic regime. The coupling is performed at the wetted surface of the float, where the seakeeping solver sends the pressure fields to the structure solver, and the latter returns structural displacements on the same surface. The time variation of structural displacements along the normal direction of the surface is imposed as a boundary condition of normal velocity on the wetted surface (see Figure 1). The use of the same technique for integrating equations in both domains -the Finite Element Method- greatly facilitates the coupling issues.

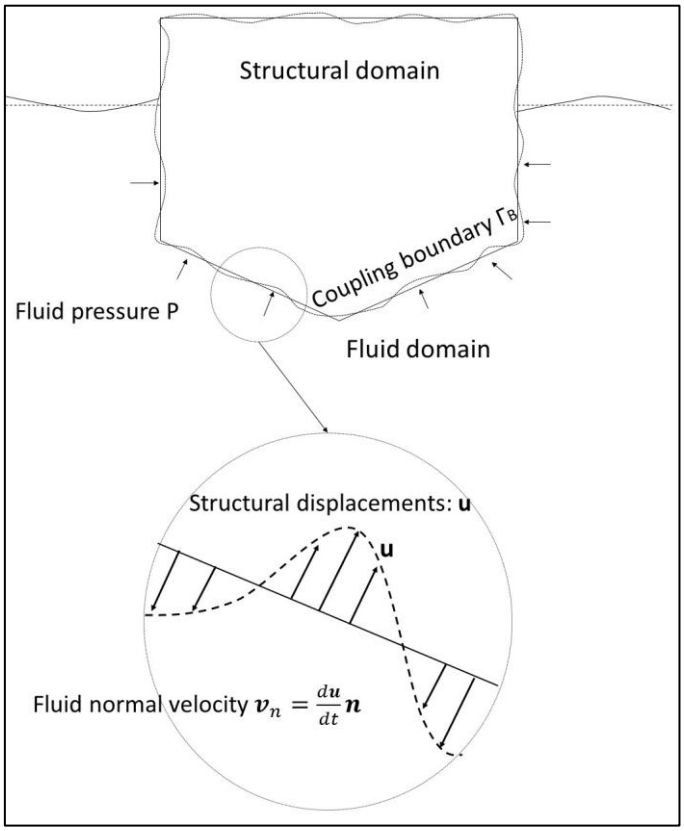

Figure 1. Fluid-structure coupling on the wetted surface of the structure.

As mentioned previously, the hydroelastic solver has been implemented in the software suite SeaFEM [4]. The core of SeaFEM [3,5,6,7,8,9,10,11,12] is a seakeeping tool that solves the wave diffraction-radiation problem in the time-domain using the Finite Element Method (FEM). SeaFEM has been developed by the Joint Research Unit CIMNE-UPM in collaboration with Compass IS since 2009. Some of the most relevant features of SeaFEM are:

- Wave diffraction-radiation solver up to second order.
- Multibody dynamics, including body links (ball joints, revolute joints, etc).
- Coupling with Open-FAST (single and multiturbine floating platforms).
- Dynamic hydro-elastic simulations (iterative and monolithic coupling; one-way and two-ways coupling and based on modal superposition).
- Mooring capabilities: spring, elastic catenary, dynamic mooring based on non-linear FEM formulation; multi-segment lines with intermediate weight and buoys; different types of seabeds.

- Coupling with Simulink.
- SeaFEM is free for non-commercial purpose, such as research and academia.

Despite the satisfactory results obtained, the computational cost of the proposed approach is very high for many practical applications. A subsequent work presented an evolution of [1], aiming to reduce the calculation time of the problem by several orders of magnitude. This reduction is achieved by projecting the FEM structural solution onto a reduced modal basis (modal order reduction) and solving the structural dynamics problem using a modal superposition strategy [2]. The fluid-structure coupling algorithm is based on the 'two-ways coupling' presented in [1].

1.2. Mode superposition method

The main idea behind this approach is to accurately approximate the solution of a detailed three-dimensional FEM model by projecting it onto a solution subspace with considerably fewer dimensions (number of degrees of freedom) compared to the original problem. The solution subspace is constructed using the modal matrix reduction technique (MMR), where the projection subspace is formed from the base vectors obtained through modal analysis [2]. We start from the classical equation of structural dynamics using the finite element method:

$$\mathbf{M}\ddot{\boldsymbol{U}}(t) + \mathbf{C}\dot{\boldsymbol{U}}(t) + \mathbf{K}\boldsymbol{U}(t) = \boldsymbol{R}(t) \tag{1}$$

Where $\mathbf{M}$, $\mathbf{C}$, $\mathbf{K}$ y $\boldsymbol{R}$ are the mass, damping, stiffness matrices, and the vector of external forces, respectively. $\boldsymbol{U}(t)$ is the vector of nodal displacements -and rotations, if applicable. The dimension of the problem is n -number of unknowns. We perform a transformation of the displacement vector $\boldsymbol{U}(t)$, given by:

$$\boldsymbol{U}(t) = \mathbf{P} \cdot \boldsymbol{X}(t) \tag{2}$$

Where $\mathbf{P}$ is a square matrix of size n x n and $\boldsymbol{X}(t)$ is a vector of size n. The components of $\boldsymbol{X}(t)$ are commonly referred to as generalized displacements. If we substitute the above relationship into the equation of elastic solid dynamics, and pre-multiply by $\mathbf{P}^{\boldsymbol{t}}$, we get:

$$\widetilde{\mathbf{M}}\ddot{\boldsymbol{X}}(t) + \widetilde{\mathbf{C}}\dot{\boldsymbol{X}}(t) + \widetilde{\mathbf{K}}\boldsymbol{X}(t) = \widetilde{\boldsymbol{R}}(t) \tag{3}$$

With $\widetilde{\mathbf{M}} = \mathbf{P}^{\boldsymbol{t}}\mathbf{M}\mathbf{P}$, $\widetilde{\mathbf{C}} = \mathbf{P}^{\boldsymbol{t}}\mathbf{C}\mathbf{P}$, $\widetilde{\mathbf{K}} = \mathbf{P}^{\boldsymbol{t}}\mathbf{K}\mathbf{P}$, $\widetilde{\boldsymbol{R}} = \mathbf{P}^{\boldsymbol{t}}\boldsymbol{R}$. The aim of this transformation is to obtain matrices with a lower bandwidth, which facilitates solving the problem. An effective method to find the transformation is to use the solution of the free vibration equations:

$$\mathbf{M}\ddot{\boldsymbol{U}}(t) + \mathbf{K}\boldsymbol{U}(t) = \mathbf{0} \tag{4}$$

The general solution can be written as:

$$\boldsymbol{U = \phi\, sin[\omega(t - t_0)]} \tag{5}$$

Where $\boldsymbol{\phi}$ is a vector of order n, and ω is a constant identified with the vibration frequency. If we substitute the above solution into the free vibration equation, we have:

$$[\mathbf{M^{-1}K}]\boldsymbol{\phi} = \omega^2\boldsymbol{\phi} \tag{6}$$

This eigenvalue problem leads to the n solutions $(\omega_1, \boldsymbol{\phi}_1)$, $(\omega_2, \boldsymbol{\phi}_2)$, …, $(\omega_n, \boldsymbol{\phi}_n)$. The eigenvectors $\boldsymbol{\phi}_i$ are orthonormal with respect to $\mathbf{M}$, that is:

$$\boldsymbol{\phi}_i^T\mathbf{M}\boldsymbol{\phi}_j \begin{cases} = \mathbf{1}\ if\ i = j \\ = \mathbf{0}\ if\ i \neq j \end{cases} \tag{7}$$

If we define the matrix $\boldsymbol{\Phi}$ containing all the eigenvectors $\boldsymbol{\phi}_i$ (referred to as vibration modes), we can write:

$$\boldsymbol{\Phi} = [\boldsymbol{\phi}_1, \boldsymbol{\phi}_2, \ldots, \boldsymbol{\phi}_n] \tag{8}$$

$$[\mathbf{M^{-1}K}]\boldsymbol{\Phi} = \boldsymbol{\Phi\Omega^2} \tag{9}$$

$$\boldsymbol{\Omega^2} = \begin{bmatrix} \omega_1^2 & 0 & 0 \\ 0 & \ddots & 0 \\ 0 & 0 & \omega_n^2 \end{bmatrix} \tag{10}$$

Where $\boldsymbol{\Omega^2}$ is a diagonal matrix. It holds true that:

$$\boldsymbol{\Phi}^T\mathbf{M}\boldsymbol{\Phi} = \mathbf{I} \tag{11}$$

$$\boldsymbol{\Phi}^T\mathbf{K}\boldsymbol{\Phi} = \boldsymbol{\Phi}^T\mathbf{M}\boldsymbol{\Phi\Omega^2} = \boldsymbol{\Omega^2} \tag{12}$$

Therefore, the matrix $\boldsymbol{\Phi}$ is suitable for the initial transformation goal. In fact, if $\boldsymbol{U}(t) = \boldsymbol{\Phi} \cdot \boldsymbol{X}(t)$, then, the equation of structural dynamics becomes:

$$\ddot{\boldsymbol{X}}(t) + \boldsymbol{\Phi}^T\mathbf{C}\boldsymbol{\Phi}\dot{\boldsymbol{X}}(t) + \boldsymbol{\Omega^2 X}(t) = \boldsymbol{\Phi}^t\boldsymbol{R}(t) \tag{13}$$

It should be clarified that, up to this point, no simplification has been made in the problem. It has merely changed the basis to the so-called Modal Generalized Displacements. Since mathematically the same space is spanned by the n eigenvectors as by the n nodal point finite element displacements, the same solution is obtained in both analyses. Therefore, the resulting equation is equivalent to the original one [13].

It is common practice to model the damping matrix of the structure using the Rayleigh model:

$$\mathbf{C} = \eta\mathbf{M} + \delta\mathbf{K} \tag{14}$$

Where η, δ are constants. Then, the structural dynamics equation can be re-written as follows:

$$\ddot{\boldsymbol{X}}(t) + \left[\eta + \delta\boldsymbol{\Omega^2}\right]\dot{\boldsymbol{X}}(t) + \boldsymbol{\Omega^2 X}(t) = \boldsymbol{\Phi^t R}(t) \tag{15}$$

η, δ parameters are defined to consider a critical damping ratio between 1% - 3% for the lower frequency modes. It is worth noting that the critical damping ratio and tends to increase for the higher vibration modes.

The above system of equations is diagonal (i.e., the equation corresponding to each mode is decoupled). Thus, the equation corresponding to the i-th mode is of the form:

$$\ddot{q}_i + c_i\dot{q}_i + \omega_i^2 q_i = f_i(t) \tag{16}$$

This is the equation for the amplitude of the i-th mode of the structure, which can be straightforwardly solved using numerical schemes such as Newmark or similar ones. Once the modal amplitude evolution is known, the displacement field can be recovered as:

$$\boldsymbol{U}(t) = \boldsymbol{\Phi} \cdot \boldsymbol{X}(t) = \sum q_i(t)\,\boldsymbol{\phi}_i \tag{17}$$

1.3. Modal Matrix Reduction

The method of mode superposition provides a perfect framework for reducing the order (number of degrees of freedom) of the problem, while retaining a high accuracy for practical purposes. The essence of that order reduction is that usually only a small fraction of the total number of decoupled equations needs to be considered in order to obtain an accurate approximation to the exact solution. Most frequently, only the first m equilibrium equations -corresponding to the lower frequency modes- need to be considered (where m << n) [2].

Based on the reference Bathe's book [13], in general, any finite element analysis approximates the lowest exact frequencies best, and little or no accuracy can be expected in approximating the higher frequencies and mode shapes. Therefore, there is usually little justification for including the dynamic response in the mode shapes with the high frequencies in the analysis. In practice, if the highest frequency of the applied loads is ω_l, then the finite element mesh should at most represent accurately the frequencies $\omega \leq 4 \cdot \omega_l$ of the actual system (dynamic response range). There is no need to represent the higher frequencies of the actual physical system accurately in the finite element system because the dynamic response contribution in these frequencies is negligible; i.e., for modes of larger frequencies, an almost static response is obtained [13],

1.4. Traditional versus new strategy

The common way to carry coupled hydroelastic analysis is shown in Figure 2. Usually, a frequency-domain seakeeping solver based on the boundary element method (BEM) is used to solve the wave diffraction-radiation problem. From this software, frequency dependent added mass, damping, diffraction and Froude-Krylov loads, and diffraction-radiation pressure distribution are obtained. Then, a rigid-body time-domain simulation is carried out by transforming frequency-domain hydrodynamic loads into time-domain loads. Then a realization in the time-domain of all external loads (including hydrodynamic pressures) acting on the structure is obtained. Finally, the latter must be imported into a structural solver (usually based on FEM) to compute the structural response. It is easily observed that this approach requires the interaction of several independent software's. This is a tedious methodology which requires solving the hydroelastic problems in several stages and only allows for one way coupling, limiting this approach to rigid structures.

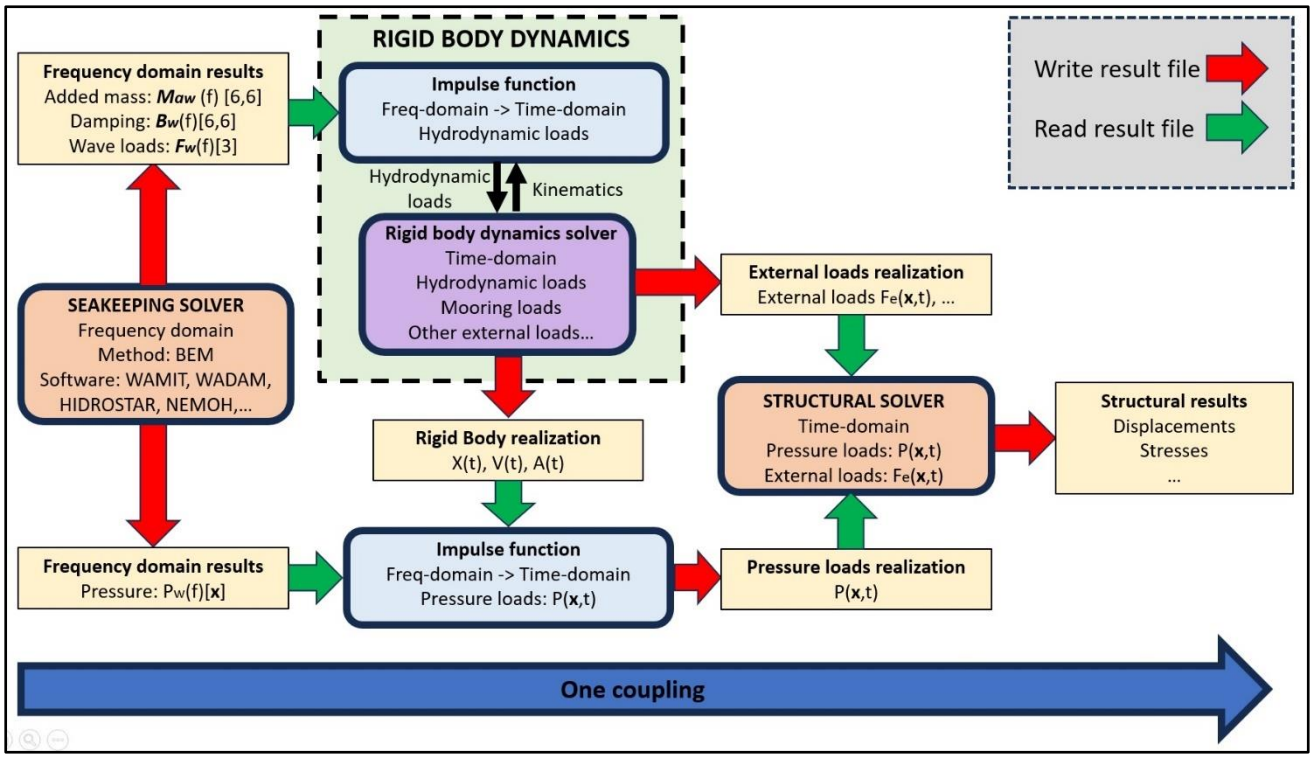

Figure 2. Conventional strategy for time-domain hydroelasticity analysis.

Figure 3 shows the new methodology proposed in this work, based on SeaFEM, a numerical framework for seakeeping. In this approach, the structural properties are extracted from a structural FEM solver. At this point, two approaches can be taken:

- FEM coupled analysis: Extract the FE mass $\mathbf{M}$ and stiffness $\mathbf{K}$ matrices.

- MMR analysis: Extract the structural eigenmodes and modal frequencies.

SeaFEM computes the external load vector for the structural problem. And once the structural properties are sent to to SeaFEM, the seakeeping and structural problems are solved simultaneously in each time-step under the same programming framework, so communication is carried out at code level (no need to write and read files during the hydroelastic execution). Moreover, two-ways coupling is enabled since the structural displacement can be added to the rigid body movements to imposed the corresponding body boundary condition in the wave diffraction-radiation solver. It can be observed that this new methodology is more straightforward and reduce the communication among different softwares.

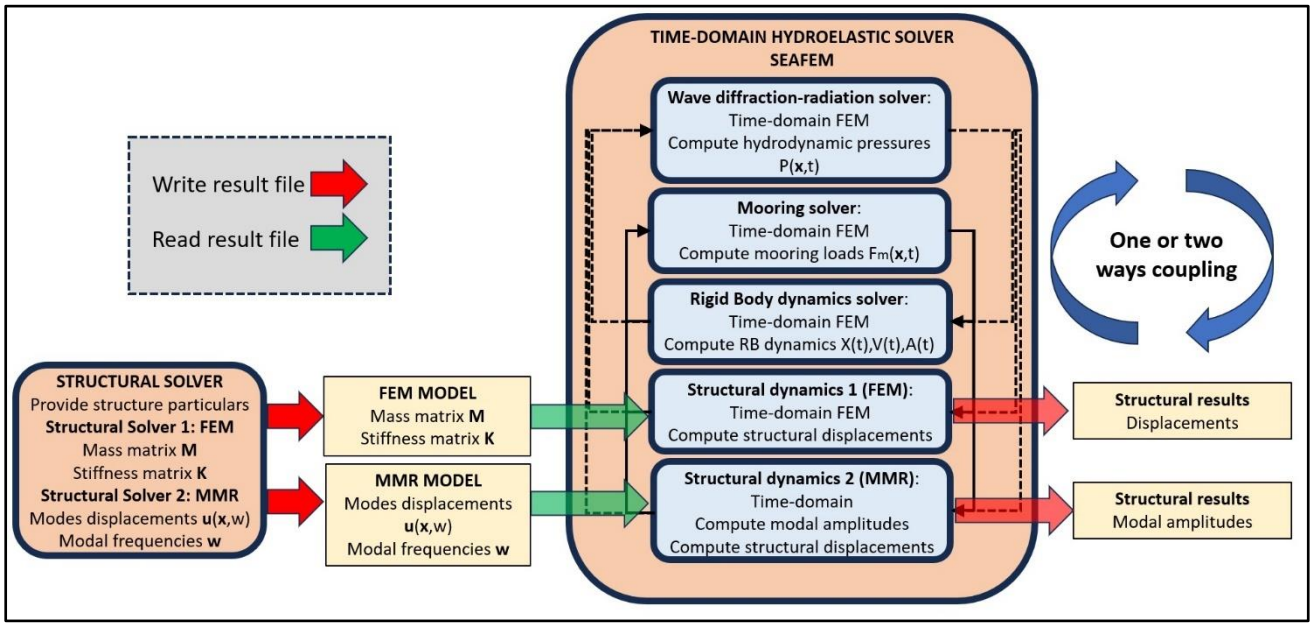

Figure 3. New strategy for time-domain hydroelasticity analysis.

The aforementioned time-domain hydroelastic simulation provides, as a result:

- FEM coupling: the time history of the structural displacements and energy
- MMR coupling: the time history of modal amplitudes and energy.

From this outputs, structural stresses can be obtained offline (no need to be computed on the fly). For instance, time steps with highest structural strain energy can be used to compute the largest stresses for the specific realization, and identify potential hotspots for fatigue failure. And full time-history of stresses can be computed at those hot-spots for fatigue analysis. This way, postprocessing time can be optimized.

2. CASE STUDY

2.1. Model description

Next a case study is proposed. Figure 4 shows the FEM mesh of the ship used as a case study, and Table 1 provides the main particulars.

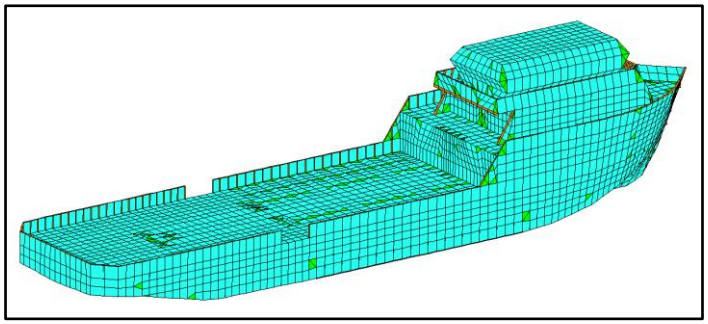

Figure 4. FEM mesh of case study.

Table 1. Case study particulars.

Displacement	1153 t
Overall length	50.292 m
Overall beam	11.03 m
Draft	3.06 m
Number of FE	19130
Number of nodes	9036
Number of degrees of freedom	54216

The structural is built in Ansys software and uses shell quadrilateral and triangular elements and beam elements. Specifically, it is composed of 11223 shell elements and 7907 beam elements. Triangular elements are only used when the geometry requires it, as Ansys always recommends the use of square elements. The model takes into account both the mass of the structure itself and the distribution of weights on board, distributed in the nodes that represent the mesh. The quality of the mesh is checked, obtaining an average shell element quality of 91%, with 78% of the elements having a quality higher than 80%.

The hydrodynamic model is based on SeaFEM. It uses the FEM to solve the wave diffraction-radiation equation. The Neumann flow linearization has been used along with the FEM-SUPG scheme to

integrate the free surface equations. Also, the transform stern flow option is activated to impose the condition of dry transom stern. The minimum element size on the free surface is 0.16m, and the time step used for stability conditions is 0.025s. The FE mesh consists of 680006 tetrahedra elements. Figure 4 shows the computational domain and FE mesh used in SeaFEM to solve the hydrodynamic problem.

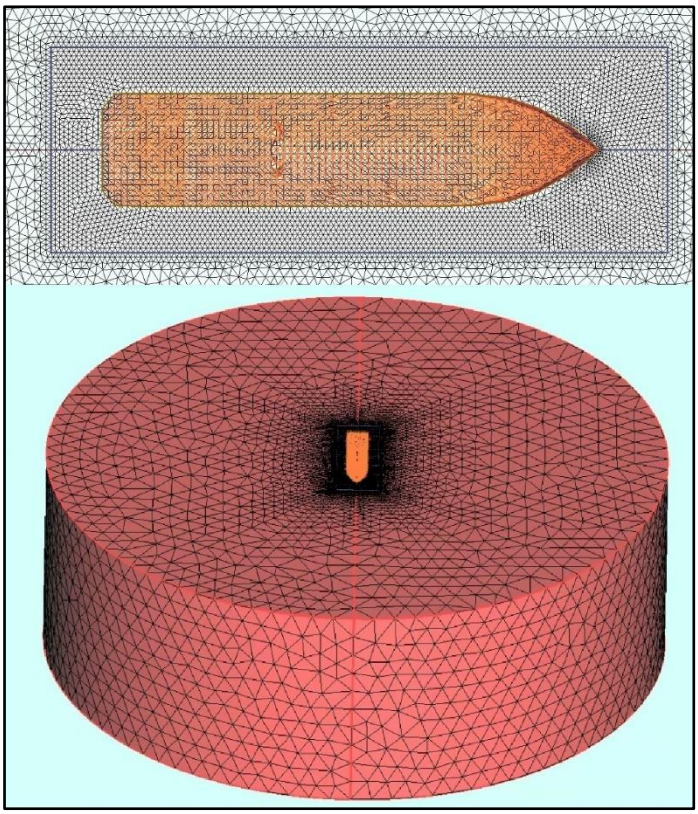

Figure 5. SeaFEM mesh and computational domain.

2.2. Modal analysis

Once a FEM structural model is built, the first step to carry out a hydroelastic analysis based on MMR is to carry out a modal analysis. This modal analysis will be carried out with the model free (no restrictions), and for the first 1000 modes. The first six modes have null modal frequency and correspond to the rigid body displacements. For the elastic modes, the rage of frequencies goes from 4.62 Hz to 68.31 Hz. Figure 6 shows the first 6 elastic modes and their modal frequencies. These frequencies are “dry” frequencies as they are computed by the structural FEM with no considerations of the presence of the water.

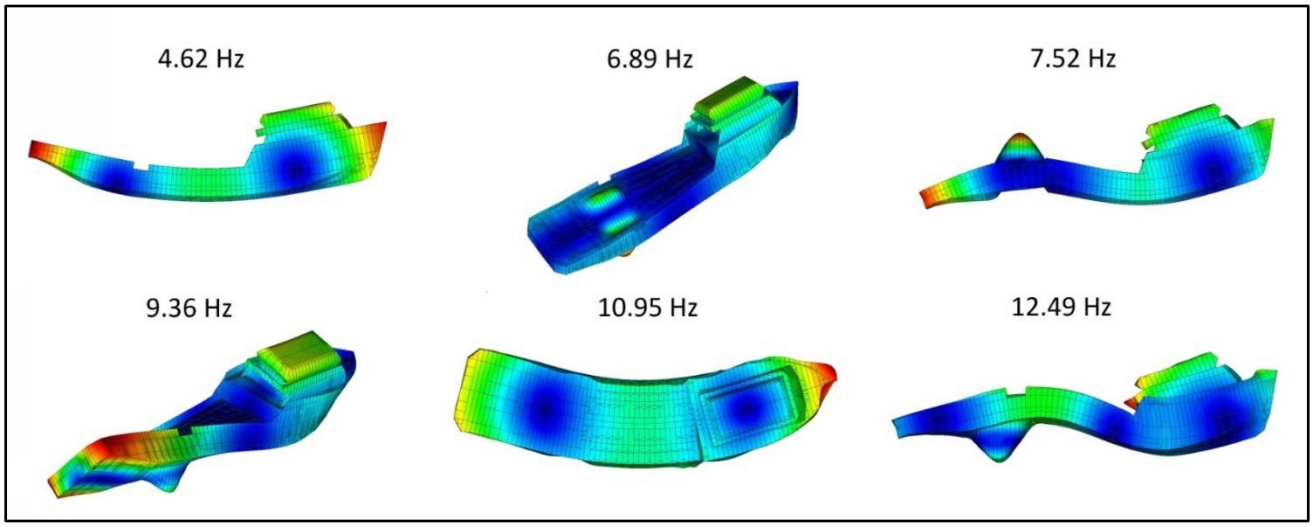

Figure 6. First elastic modes and dry modal frequencies.

If the presence of the water is considered, then: first, the structural displacement radiates waves that induced added mass and damping to the modal dynamic; second, the change in hydrostatic pressures also induced structural stiffening. This leads to a change of the modal frequencies. In order to compute this change, extinction tests are carried out for the first six modes using the 2-ways hydroelastic coupling proposed in this work, which requires solving the wave radiation problem in the time domain.

Figure 7 left shows the time evolution of the first mode extinction test, while Figure 7 right shows a snapshot of the waves radiated during the extinction test. It is observed that the wave radiation induces a change of modal period from 0.216 seconds to 0.275 seconds, and also induces a significant amount of damping. Table 2 provides the change in modal frequency for the first six elastic modes.

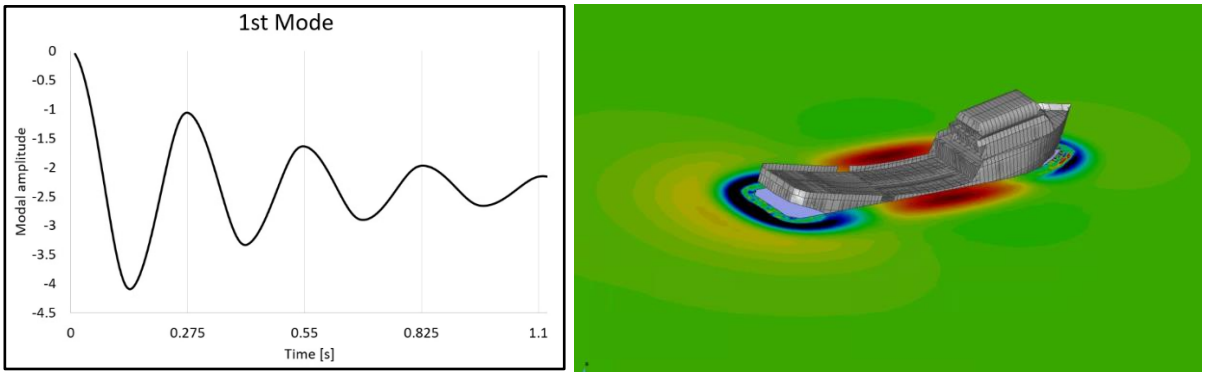

Figure 7. Extinction test for first elastic mode. Left: time evolution of modal amplitude; Right: Radiate waves.

Table 2. Change in modal frequencies.

Mode	1st Mode	2nd Mode	3rd Mode	4th Mode	5th Mode	6th Mode
Dry freq.	4.62 Hz	6.891 Hz	7.52 Hz	9.36 Hz	10.95 Hz	12.48 Hz
Wet freq.	3.64 Hz	6.37 Hz	6.29 Hz	8.24 Hz	10.00 Hz	9.71 Hz
Dry period	0.216 s	0.145 s	0.133 s	0.107 s	0.091 s	0.080 s
Wet period	0.275 s	0.157 s	0.159 s	0.121 s	0.100 s	0.103 s

2.3. Equilibrium analysis

In this section a static analysis under the hydrostatic pressure and self-weight loads is carried out. The MMR solution using 1000 modes is compared to that obtained using FEM. When using FEM, the total elastic energy of the structure is 4899.5 J, while with the MMR approximation is 4719.2 J, which represents the 96.3 % of the total energy.

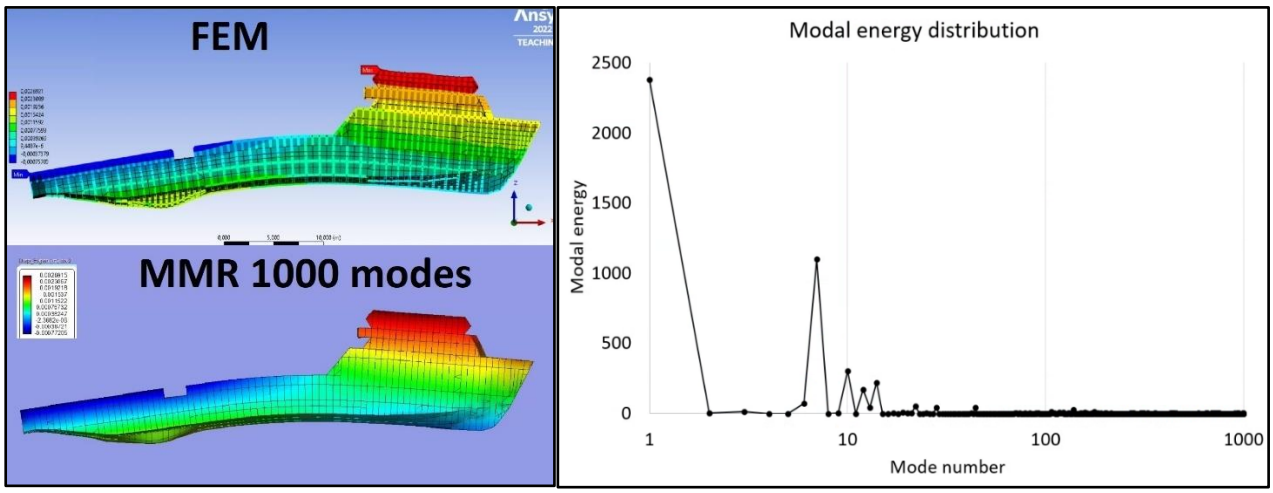

Figure 8. Hydrostatic equilibrium condition. Left: FEM vs MMR structural displacements; Right: modal energy distribution.

2.4. Energy analysis

Next, a structural analysis is performed when the ship is navigating with an operational forward speed of 10kn. Table 3 provides the operational condition under which simulated using the hydroelastic MMR model with 1000 modes. Since the dynamic response is considered to depend linearly respect to wave amplitudes, only one wave significant wave height (Hs) is needed to be simulated. Then, for other values of Hs, the instantaneous dynamic modal amplitude just needs to be scaled.

Table 3. Operational conditions simulated.

Forward speed: V	10 kn						
Wave height: Hs	1 m						
Wave Periods: T	3s	5s	7s	9s	11s	13s	15s
Wave directions	0º	30º	60º	90º	120º	150º	180º

To illustrate a modal energy analysis, the condition with 5 seconds wave period and 30º wave direction is considered. Figure 9 shows the instantaneous elastic energy of the structure during a 10 minutes simulation. Tracking the elastic energy allows for pinpointing those specific time instants where the structure is most stressed, so that reducing so the number of instants to postprocess in order to determine the maximum stresses achieved under this specific condition. Table 4 provides the values of the maximum energy for each condition analysed, which helps to identify most demanding conditions from a structural point of view.

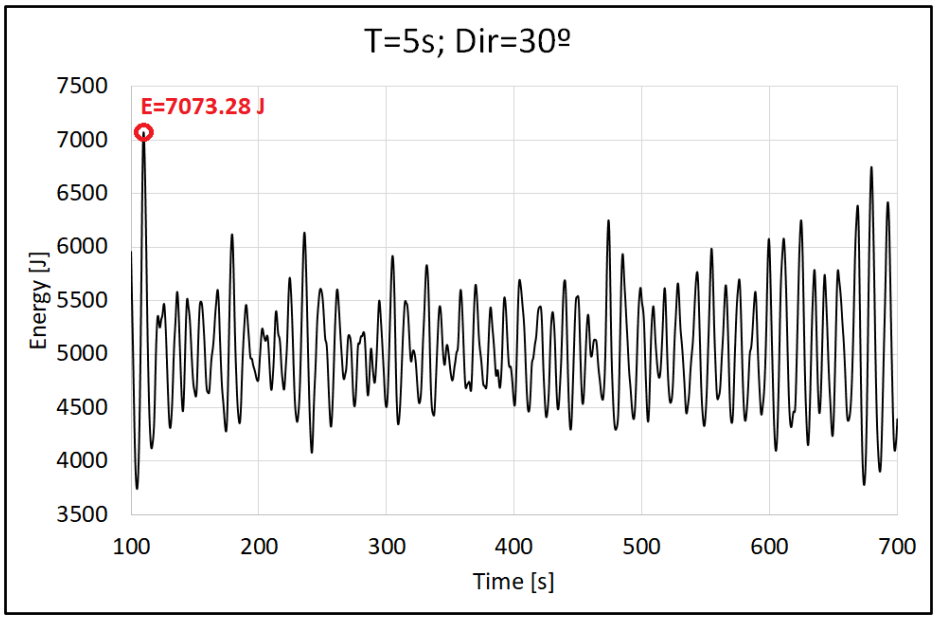

Figure 9. Instantaneous structural energy for T=5s and Dir=30º.

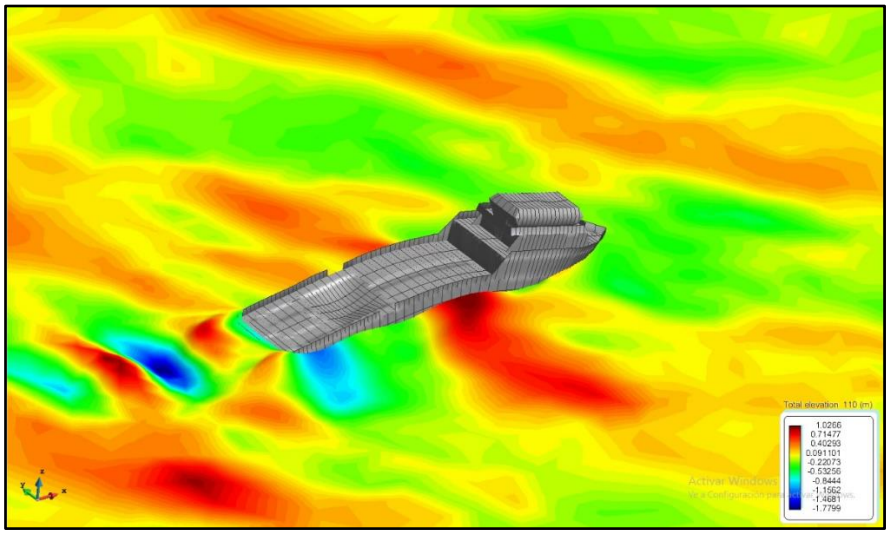

Figure 10. Snapshot for Hs=1m T=5s and Dir=30º at maximum energy instant. Colormap: free surface elevation; Structural deformation amplified by x500.

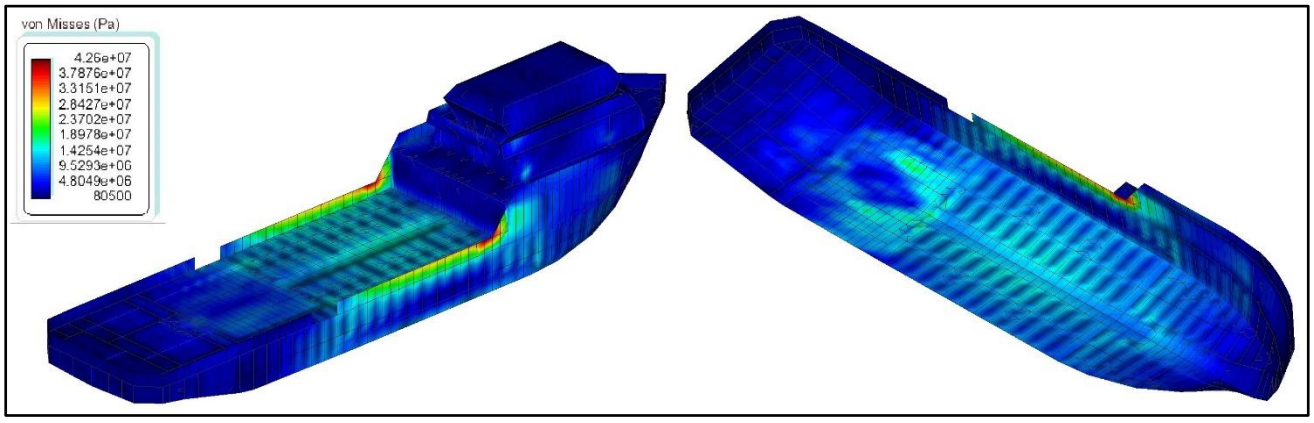

Figure 11. Snapshot for Hs=1m, T=5s and Dir=30º at maximum energy instant. Colormap: von Misses stresses.

Table 4. Maximum instantaneous structural energy.

Maximum energy [J]		T						
		3s	5s	7s	9s	11s	13s	15s
Dir	0º	5809.13	6236.33	5832.86	5787.54	5555.77	5325.36	5310.51
	30º	5869.33	7073.28	5918.39	5736.62	5432.02	5501.83	5231.48
	60º	5775.61	5882.08	5829.6	5493.7	5323.75	5253.67	5177.92
	90º	6047.47	5841.37	5757.1	5347.91	5260.08	5166.25	5163.02
	120º	6120.32	5925.14	5630.07	5429.17	5260.35	5183.7	5153.17
	150º	5982.7	6043.11	5781.66	5504.82	5385.88	5218.82	5211.26
	180º	5857.81	6101.04	5805.98	5645.92	5397.59	5336.52	5225.54

Figure 12 shows the mean and maximum modal energy distribution during the simulation. It is observed that most energetic modes tend to accumulate towards the lower frequency modes. Table 5 shows the ten most energetic modes. With only ten modes, some 95% of the energy is recovered. And only the first mode contains 42.83% of the energy. This confirms that using the MMR approximation can provide accurate solutions for dynamic structural analysis with a large reduction of the computational cost.

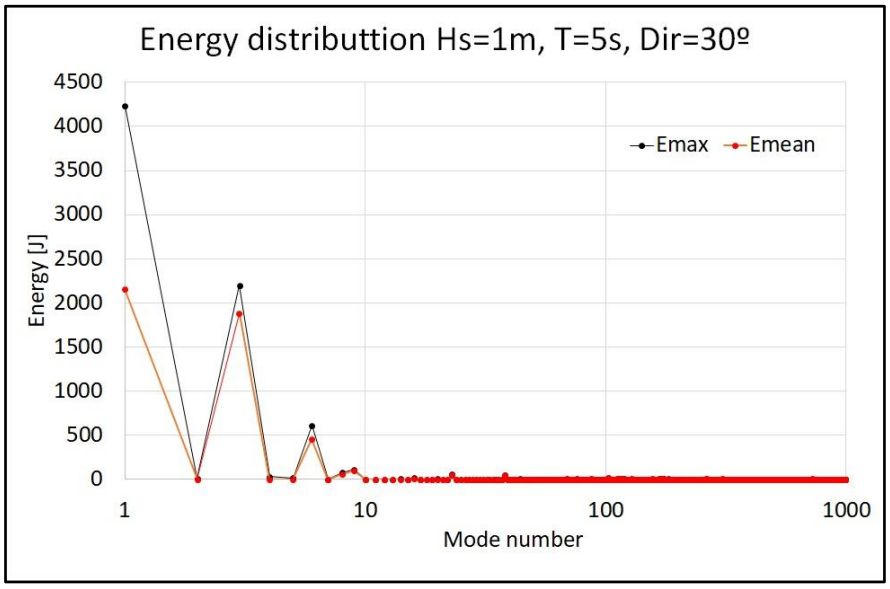

Figure 12. Maximum and mean modal energy distribution for T=5s and Dir=30º.

Table 5. Mean modal energy distribution for T=5s and 30º.

	Mode number	Modal E	Cumulative E
1	1	42.83%	42.83%
2	3	37.23%	80.06%
3	6	9.08%	89.14%
4	9	1.92%	91.06%
5	8	1.09%	92.14%
6	23	1.07%	93.21%
7	38	0.93%	94.14%
8	103	0.33%	94.48%
9	16	0.24%	94.72%
10	128	0.23%	94.95%

2.5. Fatigue analysis

For every operational condition analysed, the hydroelastic analysis provide the instantaneous modal amplitude for each mode considered and every time step. Hence, given a hot spot of the structure, the stress tensor can be easily obtained just by linear combination of the modal stresses at that point. Then, using the rain-flow counting algorithm in the time evolution of the stresses at the hot spot, the cycle counting and stress levels are obtained.

The rain-flow method counts load cycles based on how stresses vary over time. First, the algorithm identifies peaks and valleys in the stress data, then matches them up to identify load cycles. The cycles are counted according to the sequences of changes in the stress data, grouped by stress ranges, and filtered based on their amplitude and the number of times they occur. Finally, using the SN curve of the material shown in Table 6, the fatigue damage for the operational condition is obtained.

Table 6. Design S-N curve selected from BV.

Curve	FAT	1st slope		Two slope intersection		2nd slope		Reference thickness	Thickness exponent
	ΔS (MPa)	m1	$Log_{10}(K_1)$	N cycles	ΔS_q (MPa)	m2	$Log_{10}(K_2)$	t_{ref} (mm)	n
B	150.00	4.0	15.0060	10^7	100.35	7	21.0105	25	0.1

Figure 13 shows the location of node 718, on the main deck and amidships, selected for fatigue analysis. A concentration factor of 3 has been considered, simulating an opening in the deck. Figure 14 shows the instantaneous von Misses stresses at node 718, and the instantaneous structural energy, for Hs=1m, T=5s and 30º wave direction. It is observed how both results correlates, confirming that using the energy criterion is useful to identify those instants with highest structural energy and highest stresses. The instantaneous stresses time history is what is needed to perform the fatigue analysis.

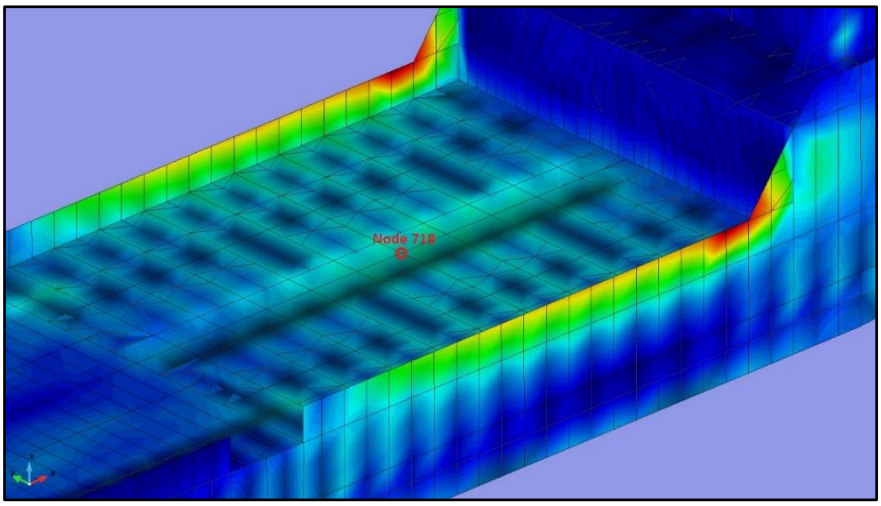

Figure 13. Location of node 718 for fatigue analysis.

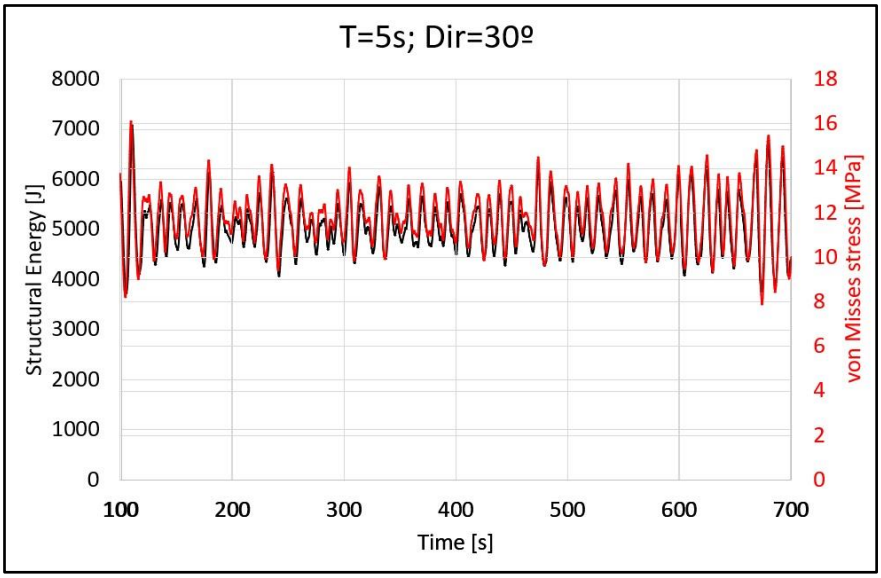

Figure 14. Instantaneous von Misses stresses at node 718 and structural energy for Hs=1m, T=5s, and Dir=30º.

Table 7 provides an example of the probability of occurrence of a specific seastate at a given location. Table 8 provides the estimated annual accumulated damage for wave period T=5s and different values of Hs and wave directions. In this analysis, the wave direction is considered relative to the ship course, and to be equally probable. Hence the average damage is obtained by weighting the damage for each direction. Table 9 provides the estimated annual fatigue damage for the seastates of Table 7. Multiplying, for each pair (Hs,T), the probability of occurrence in Table 7 by the mean damage in Table 9 we obtained the estimated mean annual fatigue damage in Table 10.

Table 7. Seastate annual probability particulars (year 2023) at SIMAR 2120096. Source: Puertos del Estado

Annual Probability [%]		T					
		3s	5s	7s	9s	11s	13s
Hs	1m	1.635	26.300	18.615	6.385	1.741	0.083
	2m	0	3.586	10.327	10.773	4.970	0.713
	3m	0	0.021	1.520	5.787	2.217	0.466
	4m	0	0	0.021	1.273	1.599	0.110
	5m	0	0	0	0.095	0.991	0.184
	6m	0	0	0	0	0.252	0.084
	7m	0	0	0	0	0.047	0.047
	8m	0	0	0	0	0.016	0.142

Table 8. Estimated annual fatigue damage (year 2023) at SIMAR 2120096 for T=5s.

T=5s Annual fatigue damage [0-1]		Direction (º)							Average value (equi-probable directions)
		0º	30º	60º	90º	120º	150º	180º	
Hs	1m	7.01E-08	5.26E-07	1.59E-08	2.02E-08	1.25E-08	2.85E-08	4.87E-08	1.10E-07
	2m	8.49E-06	6.43E-05	1.96E-06	2.33E-06	1.87E-06	3.46E-06	6.10E-06	1.35E-05
	3m	1.35E-04	9.89E-04	2.79E-05	4.42E-05	3.66E-05	5.28E-05	9.53E-05	2.11E-04
	4m	8.30E-04	3.20E-03	2.00E-04	3.46E-04	3.47E-04	3.72E-04	6.92E-04	8.72E-04
	5m	2.44E-03	1.00E-02	6.80E-04	1.62E-03	1.91E-03	1.61E-03	2.91E-03	3.09E-03
	6m	6.18E-03	2.43E-02	2.27E-03	4.65E-03	7.75E-03	5.01E-03	8.30E-03	8.53E-03
	7m	1.29E-02	4.80E-02	5.55E-03	1.07E-02	1.76E-02	1.16E-02	1.93E-02	1.83E-02
	8m	2.49E-02	8.12E-02	1.07E-02	2.39E-02	3.98E-02	2.35E-02	3.81E-02	3.51E-02

Table 9. Estimate annual fatigue damage (year 2023) at SIMAR 2120096.

Annual fatigue damage [0-1]		T					
		3s	5s	7s	9s	11s	13s
Hs	1m	1.13E-08	1.10E-07	7.60E-09	1.67E-09	9.41E-11	3.32E-11
	2m	1.38E-06	1.35E-05	8.94E-07	2.11E-07	1.21E-08	4.24E-09
	3m	2.33E-05	2.11E-04	1.51E-05	3.55E-06	2.07E-07	7.22E-08
	4m	1.59E-04	8.72E-04	1.03E-04	2.55E-05	1.53E-06	5.38E-07
	5m	7.30E-04	3.09E-03	4.35E-04	1.18E-04	7.23E-06	2.54E-06
	6m	2.24E-03	8.53E-03	1.45E-03	3.99E-04	2.56E-05	9.12E-06
	7m	5.63E-03	1.83E-02	3.46E-03	9.94E-04	7.42E-05	2.63E-05
	8m	1.16E-02	3.51E-02	7.06E-03	2.10E-03	1.83E-04	6.59E-05

Table 10. Estimated mean annual fatigue damage (year 2023) at SIMAR 2120096.

Mean Annual fatigue damage [0-1]		T						
		3s	5s	7s	9s	11s	13s	
Hs	1m	1.85E-10	2.90E-08	1.42E-09	1.07E-10	1.64E-12	2.76E-14	3.08E-08
	2m	0	4.86E-07	9.24E-08	2.27E-08	6.00E-10	3.02E-11	6.01E-07
	3m	0	4.43E-08	2.29E-07	2.05E-07	4.58E-09	3.37E-10	4.84E-07
	4m	0	0	2.16E-08	3.25E-07	2.44E-08	5.92E-10	3.72E-07
	5m	0	0	0	1.12E-07	7.17E-08	4.68E-09	1.89E-07
	6m	0	0	0	0	6.46E-08	7.66E-09	7.23E-08
	7m	0	0	0	0	3.49E-08	1.24E-08	4.72E-08
	8m	0	0	0	0	2.93E-08	9.36E-08	1.23E-07
		1.85E-10	5.59E-07	3.45E-07	6.66E-07	2.30E-07	1.19E-07	1.92E-06

3. CONCLUSIONS

In this work, a novel strategy for simulating hydroelastic is presented. This strategy is based on the direct simulation in the time-domain of the seakeeping hydrodynamics problem coupled with the structural problem. One of the key points is the used of the MMR to reduce the computational cost of solving the structural dynamic problem. This strategy presents the following advantages:

- Allows one-way and two-ways coupled hydroelastic simulations.
- Hydroelastic problem solved under the same programming framework, reducing overheads from communication/data exchange among different softwares.
- Drastic reduction of CPU time by using MMR instead of solving the full FEM.

- Drastic reduction of outputs by using MMR (only modal amplitudes are recorded for the whole simulation).
- Capabilities to compute modal RAOs (MRAOs).

The present hydroelastic framework has been applied to analyse the structural response of a ship under specific operational conditions and to demonstrate the capabilities of the present methodology.

4. FUTURE WORK

The present work is currently ongoing under MLAMAR and Fibregy projects. In order to be able to perform a more extensive analysis under any operative conditions, modal amplitude respond operators (MRAOs) could be obtained under the linear problem assumptions.

In order to obtain the MRAO, a number of white noise analysis for different wave trains along all directions and for different cruise speed must be performed. If wave directions are taken every 10º, thanks to the symmetry of the problem, 19 directions must be analysed. If the analysis is performed for Froude numbers from 0 to 0.3 every 0.5, then 7 speed must be analysed. This results in 133 simulations. Considering an average of 24 CPUxh per analysis, these results will require some 3192 CPUxh. If a work station with 32 cpus is used, the MRAOs could be obtained in about 100 hours. Once the MRAOS are obtained for the previous conditions, any intermediate condition can be accurately interpolated, providing the MRAOs for any seawaves at any navigating speed. Hence, long modal realizations for any operational conditions can be performed very fast with no need of performing more numerical hydroelastic simulations in the time-domain. These realizations will provide the time series of the modal amplitudes, which is all need to post-process the structural response under a given operational condition.

Currently RAOs analysis is available in SeaFEM only without navigation speed. The authors are currently implementing in SeaFEM the RAOs analysis for navigation conditions in order to be able to obtain the MRAOS.

ACKNOWLEDGEMENTS

This work has been funded by “Ministerio de Ciencia e Innovacion” under grant agreement MLAMAR (ref. PID2021-126561OB-C31) and by The European Commission under grant agreements H2020 FibreGy (ref. 952966).

The structural FEM model has been taken from MAESTRO and provided by Navantia for the execution of the present study case.

REFERENCES

[1] B. Servan-Camas, D. Di-Capua, J. Garcia-Espinosa, D. Sa-Lopez, Fully 3D ship hydroelasticity: Monolithic versus partitioned strategies for tight coupling, Marine Structures, Volume 80, 2021, 103098, ISSN 0951-8339, https://doi.org/10.1016/j.marstruc.2021.103098.

[2] J. García-Espinosa; B. Serván-Camas; M. Calpe-Linares, High Fidelity Hydroelastic Analysis Using Modal Matrix Reduction. J. Mar. Sci. Eng. 2023, 11, 1168.

[3] B. Serván-Camas, J. García-Espinosa, Accelerated 3D multi-body seakeeping simulations using unstructured finite elements, Journal of Computational Physics, Volume 252, 2013, Pages 382-403, ISSN 0021-9991, https://doi.org/10.1016/j.jcp.2013.06.023.

[4] Compass IS. SeaFEM Theory manual. accessed 8 March 2024. https://www.compassis.com/en/tdyn/tdyn-seafem-support/

[5] B. Servan-Camas; J.E. Gutierrez-Romero; J. Garcia-Espinosa, A time-domain second-order FEM model for the wave diffraction-radiation problem. Validation with a semisubmersible platform. Mar. Struct. 2018, 58, 278–300.

[6] J. García-Espinosa, D. Di Capua, B. Serván-Camas, P.A Ubach, E. Oñate, A FEM fluid–structure interaction algorithm for analysis of the seal dynamics of a Surface-Effect Ship, Computer Methods in Applied Mechanics and Engineering, Volume 295, 2015, Pages 290-304, ISSN 0045-7825, https://doi.org/10.1016/j.cma.2015.07.010.

[7] J. García-Espinosa; B. Serván-Camas, A non-linear finite element method on unstructured meshes for added resistance in waves. Ships Offshore Struct. 2019, 14, 153–164.

[8] J. E. Gutiérrez-Romero, A. J. Lorente-López & B. Zamora-Parra (2020) Numerical analysis of fish farm behaviour in real operational conditions, Ships and Offshore Structures, 15:7, 737-752, DOI: 10.1080/17445302.2019.1671674

[9] B. Serván-Camas, J.L. Cercós-Pita, J. Colom-Cobb, J. García-Espinosa, A. Souto-Iglesias, Time domain simulation of coupled sloshing–seakeeping problems by SPH–FEM coupling, Ocean Engineering, Volume 123, 2016, Pages 383-396, ISSN 0029-8018, https://doi.org/10.1016/j.oceaneng.2016.07.003.

[10] J. E. Gutiérrez-Romero, J. García-Espinosa, B. Serván-Camas, B. Zamora-Parra, Non-linear dynamic analysis of the response of moored floating structures, Marine Structures, Volume 49, 2016, Pages 116-137, ISSN 0951-8339, https://doi.org/10.1016/j.marstruc.2016.05.002.

[11] I. Berdugo-Parada; B. Servan-Camas; J. Garcia-Espinosa, Numerical Framework for the Coupled Analysis of Floating Offshore Multi-Wind Turbines. J. Mar. Sci. Eng. 2024, 12, 85. https://doi.org/10.3390/jmse12010085

[12] J.E. Gutiérrez-Romero; J. Esteve-Pérez, Assessment of the Influence of Added Resistance on Ship Pollutant Emissions and Freight Throughput Using High-Fidelity Numerical Tools. J. Mar. Sci. Eng. 2022, 10, 88. https://doi.org/10.3390/jmse10010088

[13] K.J Bathe. Finite Element Procedures. K. J. Bathe, Watertown, MA. ISBN 978-0-9790049-5-7